

Near-field Imaging Point-like Scatterers and Extended Elastic Solid in a Fluid

Tao Yin^{1,*}, Guanghui Hu² and Liwei Xu^{1,3}

¹ College of Mathematics and Statistics, Chongqing University, Chongqing 400044, P.R. China.

² Beijing Computational Science Research Center, Beijing 100094, P.R. China.

³ Institute of Computing and Data Science, Chongqing University, Chongqing 400044, P.R. China.

Received 9 February 2015; Accepted (in revised version) 9 September 2015

Abstract. Consider the time-harmonic acoustic scattering from an extended elastic body surrounded by a finite number of point-like obstacles in a fluid. We assume point source waves are emitted from arrayed transducers and the signals of scattered near-field data are recorded by receivers not far away from the scatterers (compared to the incident wavelength). The forward scattering can be modeled as an interaction problem between acoustic and elastic waves together with a multiple scattering problem between the extended solid and point scatterers. We prove a necessary and sufficient condition that can be used simultaneously to recover the shape of the extended elastic solid and to locate the positions of point scatterers. The essential ingredient in our analysis is the outgoing-to-incoming (Oti) operator applied to the resulting near-field response matrix (or operator). In the first part, we justify the MUSIC algorithm for locating point scatterers from near-field measurements. In the second part, we apply the factorization method, the continuous analogue of MUSIC, to the two-scale scattering problem for determining both extended and point scatterers. Numerical examples in 2D are demonstrated to show the validity and accuracy of our inversion algorithms.

AMS subject classifications: 74J25, 74J20, 35R30, 35Q74

Key words: MUSCI, near-field imaging, point sources, factorization method, inverse scattering, fluid-solid interaction problem.

1 Introduction

The time-reversal imaging with Multiple Signal Classification (time-reversal MUSIC) is well-known for signal-processing applications [12,16]. It provides a method to determine

*Corresponding author. *Email addresses:* taoyin_cqu@163.com (T. Yin), hu@csrc.ac.cn (G. Hu), xul@cqu.edu.cn (L. Xu)

one or more unknown small scatterers from the so-called multistatic response matrix by neglecting the physical properties and the geometry of the target. Several algorithms have been developed to recover extended scatterers since then. The approach proposed in [17, 38] was based on a physical factorization of the scattered field and the singular value decomposition of the response matrix for extended targets. This approach has been extended to recover point and extended scatterers from far-field patterns [5], relying on a generalized Foldy-Lax formulation proposed originally in [15, 23].

The Factorization Method [28] proposed by Kirsch (1998) can also be regarded as the continuous analogue of the MUSIC algorithm. A relation between the MUSIC and Linear Sampling Method was first investigated in [7]. In the Born approximation case where the multiple scattering between the point scatterers are neglected, the MUSIC was treated as a discrete analogue of the Factorization Method in inverse medium scattering [27]. Consequently, the range of the far-field response matrix can be used to derive a necessary and sufficient condition for precisely characterizing the positions of point scatterers. The same characterization was obtained in [8, 9] by taking into account the multiple scattering in the Foldy regime. The direct and inverse electromagnetic scattering by isotropic point-like obstacles in three dimensions were analyzed in [10], and the determination of the scattering strengths attached to point scatterers has been discussed in [8–10].

The goal of this paper is to justify the MUSIC algorithm for recovering point-like and extended scatterers from the near-field measurements generated by incident point sources. Compared to the far-field case (see e.g., [8, 9, 27] or [29, Chapter 4.1]), difficulty arises from the failure of the decomposition of the near field matrix (or operator) \mathbf{N} into the form $\mathbf{N} = \mathbf{H}^* \mathbf{S} \mathbf{H}$ (cf. Sections 2.2 and 3.1). On the other hand, it is an open problem how to factorize the near-field operator analogously to the far-field case until the recent studies of the outgoing-to-incoming (Oti) operator carried out in [21]. Following the idea of [21] we apply the Oti operator T to the near-field response matrix (or operator) and hence obtain a factorization of the form $T\mathbf{N} = \mathbf{H}^* \mathbf{S} \mathbf{H}$. Consequently, the spectrum of the modified near-field response matrix (or operator) $T\mathbf{N}$ can be used to characterize the scatterers, even in the two-scale scattering model. We emphasize that the uniqueness follows immediately from our computational criterion, because it is not only sufficient but also necessary for solving the inverse problem.

In this paper, an appropriate factorization of the near-field operator is established with the help of the ‘impedance’ boundary conditions across point-like scatterers (see (2.4)-(2.5)). These boundary conditions show that, around a point scatterer, the behavior of total field is similar to that of a point source wave, and that the coefficient of the leading (singular) term is proportional to that of the sub-leading term (that is why they look like the impedance boundary condition for extended obstacles). Our methods are closest to the recently developed imaging scheme [22] for inverse acoustic scattering by an extended sound-soft obstacle surrounded by point-like scatterers. Emphasis of this paper will be placed upon a straightforward proof of the well-posedness of direct scattering problems, providing ‘explicit’ solutions to the fluid-solid interaction problem in the two-scale model. Our mathematical analysis turns out to be more complicated and tricky

than the factorization methods developed in [22, 30, 37] for extended scatterers. This is due to the fact that one should take into account in the two-scale scattering model not only the interaction between acoustic and elastic waves but also the multiple scattering between the extended solid and point scatterers. Using the OI operator defined in [37], our scheme can be readily extended to the case where the near-field data are collected on non-spherical measurement surfaces.

Other inversion schemes for identifying extended elastic bodies were investigated in [13, 14] where an optimization-based technique was applied and in [34, 35] using the Reciprocity Gap and Linear Sampling Methods. See also [3, 4, 6, 19, 20, 25, 32] for recovering extended scatterers with near-field data or for locating small obstacles. The boundary element method has been used in [18, 33] to treat the forward FSI problem with extended solids only.

The rest of the paper is organized as following. We provide a necessary and sufficient condition for locating the point scatterers with a finite number of incident point sources in Section 2, relying on the MUSIC algorithm and the point-interaction model. Section 3 is devoted to the factorization method for the two-scale inverse scattering problem with infinitely many point source waves.

2 MUSIC algorithm with near-field measurements

2.1 Direct scattering by point-like scatterers

Assume a time-harmonic point source wave p^i is incident onto a collection of point-like small scatterers embedded in a homogeneous background medium. Denote by $k := \omega/c$ the wave number of the acoustic wave propagating in the background medium, where ω is the frequency and $c > 0$ the sound speed. Let $Y := \{y_j \in \mathbb{R}^3 : j = 1, 2, \dots, N\}$ be the set of locations of point-like obstacles, and let p^i be an incident point source wave of the form

$$p^i(x) = p^i(x, z) = \Phi_k(x, z), \quad x \in \mathbb{R}^3, \quad z \in \mathbb{R}^3 \setminus Y, \quad x \neq z,$$

where $\Phi_k(x, z)$ is the fundamental solution of the Helmholtz equation $(\Delta + k^2)u = 0$, defined by

$$\Phi_k(x, z) = \frac{e^{ik|x-z|}}{4\pi|x-z|}, \quad x \neq z.$$

Then the scattered field $p^s(\cdot, z)$ satisfies the reduced wave equation

$$\Delta p^s + k^2 p^s = 0 \quad \text{in } \mathbb{R}^3 \setminus Y \tag{2.1}$$

and the Sommerfeld radiation condition

$$\lim_{r \rightarrow \infty} r \left(\frac{\partial p^s}{\partial r} - ik p^s \right) = 0, \quad r = |x| \tag{2.2}$$

uniformly with respect to $\hat{x} = x/|x| \in \mathbb{S}^2 := \{\hat{\theta} \in \mathbb{R}^3 : |\hat{\theta}| = 1\}$. From this radiation condition it follows that the scattered field p^s has the asymptotic behavior of an outgoing spherical wave

$$p^s(x) = \frac{e^{ik|x|}}{4\pi|x|} \left\{ p^\infty(\hat{x}) + \mathcal{O}\left(\frac{1}{|x|}\right) \right\} \quad \text{as } |x| \rightarrow \infty \quad (2.3)$$

uniformly in all directions \hat{x} , where $p^\infty(\hat{x})$ defined on the unit sphere \mathbb{S}^2 is known as the far field pattern of the scattered field with the argument \hat{x} denoting the observation direction.

Let $p(\cdot, z) := p^i(x, z) + p^s(x, z)$ be the total field. In this study, the scattering effect due to the presence of point-like obstacles is modelled as point interactions. This allows us to employ the following "impedance"-type boundary condition across y_j :

$$(\Gamma_2 p)_j = \alpha_j (\Gamma_1 p)_j, \quad \alpha_j \in \mathbb{C}, \quad j = 1, 2, \dots, N, \quad (2.4)$$

where

$$(\Gamma_1 p)_j := \lim_{x \rightarrow y_j} 4\pi|x - y_j|p(x), \quad (\Gamma_2 p)_j := \lim_{x \rightarrow y_j} \left(p(x) - \frac{(\Gamma_1 p)_j}{4\pi|x - y_j|} \right). \quad (2.5)$$

By definition, the total field has the asymptotic behavior around the point scatterers as follows:

$$p(x, z) = \frac{(\Gamma_1 p)_j}{4\pi|x - y_j|} + (\Gamma_2 p)_j + o(1) \quad \text{as } x \rightarrow y_j.$$

Hence the boundary condition (2.4) implies that, the coefficient of the leading (singular) term of p is proportional to that of the sub-leading term. The 'impedance' coefficient α_j will be referred to as the scattering coefficient attached to the j -th scatterer, which physically describes the scattering strength of the scatterer. We refer to e.g. [1, 2, 31] or [22, Section 2.2] for the derivation and interpretation of (2.4) in the point-interaction model, based on the self-adjoint extension theory of the 3D Laplacian operator.

For simplicity we write $\alpha = (\alpha_1, \alpha_2, \dots, \alpha_N)$. To describe the solution of (2.1)-(2.4), we introduce the matrix $\Theta = \Theta(k, \alpha)$ with the entries

$$[\Theta]_{m,j} = \begin{cases} \Phi_k(y_m, y_j), & m \neq j, \\ \frac{ik}{4\pi} - \alpha_j, & m = j, \end{cases} \quad (2.6)$$

and define the set

$$S_\alpha := \{k > 0 : \det(\Theta(k, \alpha)) = 0\}.$$

For fixed $k > 0$, we refer to [8, 9] or [22, Remark 4.12 (i)] for the conditions imposed on α_j and y_j ensuring the invertibility of the matrix Θ .

Theorem 2.1. *Suppose that $k \notin S_\alpha$ and $\text{Im} \alpha_j \leq 0$ for all $j = 1, 2, \dots, N$. Then the unique solution to problem (2.1)-(2.4) in $H^1_{loc}(\mathbb{R}^3 \setminus Y)$ can be represented as*

$$p^s(x, z) = - \sum_{m,j=1}^N \left[\Theta^{-1}(k, \alpha) \right]_{m,j} \Phi_k(y_j, z) \Phi_k(x, y_m), \quad x, z \in \mathbb{R}^3 \setminus Y. \tag{2.7}$$

The expression of p^s follows directly from [22, Proposition 3.5] in the absence of the extended obstacle. Since the arguments of [22] are mostly devoted to a rigorous mathematical justification of the two-scale model for acoustic scattering by extended and point-like scatterer, we provide below a straightforward proof to the well-posedness of Theorem 2.1. Throughout the paper, we set $B_r(z) := \{x \in \mathbb{R}^3 : |x - z| < r\}$ and $B_R := B_R(O)$ with the boundary $\Gamma_R := \{x : |x| = R\}$.

Proof. Uniqueness. Supposing that $p^i = 0$, we need to prove $p^s = p = 0$. Choose $\epsilon > 0$ sufficiently small and $R > 0$ sufficiently large such that

$$B_\epsilon(y_j) \subset B_R, \quad B_\epsilon(y_j) \cap B_\epsilon(y_m) = \emptyset \quad \text{for all } j, m = 1, 2, \dots, N, \quad j \neq m.$$

Applying Green's second formula to p^s in the region $B_{R,\epsilon} = B_R \setminus \{\cup_{j=1}^N \overline{B_\epsilon(y_j)}\}$, we find

$$\begin{aligned} 0 &= - \int_{B_{R,\epsilon}} (\Delta p^s + k^2 p^s) \overline{p^s} dx \\ &= \int_{B_{R,\epsilon}} (|\nabla p^s|^2 - k^2 |p^s|^2) dx - \int_{\Gamma_R} \partial_\nu p^s \overline{p^s} ds + \sum_{j=1}^N \int_{\partial B_\epsilon(y_j)} \partial_\nu p^s \overline{p^s} ds, \end{aligned} \tag{2.8}$$

where the normal directions at $\partial B_\epsilon(y_j)$ or Γ_R are assumed to point outward. Since p^s satisfies the Sommerfeld radiation condition, there holds

$$\int_{|x|=R} \partial_\nu p^s \overline{p^s} ds = \frac{ik}{(4\pi)^2} \|p^\infty\|_{L^2(S^2)}^2 + o(R^{-1}) \quad \text{as } R \rightarrow \infty, \tag{2.9}$$

where p^∞ is the far-field pattern of the scattered field p^s . Next, we estimate the integral on $\partial B_\epsilon(y_j)$ in (2.8) by using the boundary condition (2.4). Setting $C_j := (\Gamma_1 p^s)_j$, we have by (2.4)

$$p^s(x, z) = \frac{C_j}{4\pi|x - y_j|} + \alpha_j C_j + \mathcal{O}(1)(|x - y_j|) \quad \text{as } x \rightarrow y_j,$$

for $j = 1, 2, \dots, N$. Then it holds on $\partial B_\epsilon(y_j)$ that

$$\partial_\nu p^s = \frac{x - y_j}{|x - y_j|} \cdot \nabla p^s = \frac{C_j}{4\pi|x - y_j|^2} + \mathcal{O}(1) \frac{x - y_j}{|x - y_j|} + \mathcal{O}(|x - y_j|) \quad \text{as } x \rightarrow y_j.$$

Applying the mean value theorem, simple calculations show that there exists a point $x_j^* \in \partial B_\epsilon(y_j)$ such that

$$\int_{\partial B_\epsilon(y_j)} \partial_\nu p^s \overline{p^s} ds = 4\pi\epsilon^2 \partial_\nu p^s(x_j^*) \overline{p^s(x_j^*)} = \frac{|C_j|^2}{4\pi\epsilon} + \alpha_j |C_j|^2 + o(\epsilon) \tag{2.10}$$

as $\epsilon \rightarrow 0$. Inserting (2.9) and (2.10) to (2.8), taking the imaginary part of the resulting expression and letting $R \rightarrow \infty, \epsilon \rightarrow 0$, we get

$$\frac{k}{(4\pi)^2} \|p^\infty\|_{L^2(S^2)}^2 - \sum_{j=1}^N \text{Im}(\alpha_j) |C_j|^2 = 0. \tag{2.11}$$

This together with the assumption $\text{Im}\alpha_j \leq 0$ yields $p^\infty = 0$ on S^2 . By Rellich’s lemma, we obtain $p^s = 0$ in $\mathbb{R}^3 \setminus Y$ which proves uniqueness.

Existence. We need to verify that the solution of the form (2.7) satisfies (2.1)-(2.4). For this purpose it suffices to check the boundary condition (2.4). From the definition of Γ_1 and Γ_2 , we know

$$(\Gamma_2 \Phi_k(x, y))_j - \alpha_j (\Gamma_1 \Phi_k(x, y))_j = \begin{cases} \Phi_k(y_j, y), & y \in \mathbb{R}^3 \setminus Y, \\ \Phi_k(y_j, y_m), & y = y_m \in Y, m \neq j, \\ \frac{ik}{4\pi} - \alpha_j, & y = y_j \in Y. \end{cases} \tag{2.12}$$

This implies that

$$(\Gamma_2 \Phi_k(x, y_m))_j - \alpha_j (\Gamma_1 \Phi_k(x, y_m))_j = \Theta_{m,j}, \quad m, j = 1, 2, \dots, N.$$

By direct computing, we have for $j = 1, 2, \dots, N$,

$$\begin{aligned} & (\Gamma_2 p(\cdot, z))_j - \alpha_j (\Gamma_1 p(\cdot, z))_j \\ &= \Phi_k(y_j, z) + (\Gamma_2 p^s(\cdot, z))_j - \alpha_j (\Gamma_1 p^s(\cdot, z))_j \\ &= \Phi_k(y_j, z) - \sum_{m,l=1}^N \Phi_k(y_l, z) \left[\Theta^{-1}(k, \alpha) \right]_{m,l} \left[(\Gamma_2(\Phi_k(\cdot, y_m)))_j - \alpha_j (\Gamma_1(\Phi_k(\cdot, y_m)))_j \right] \\ &= \Phi_k(y_j, z) - \sum_{l=1}^N \left[\sum_{m=1}^N [\Theta(k, \alpha)]_{j,m} \left[\Theta^{-1}(k, \alpha) \right]_{m,l} \right] \Phi_k(y_l, z) \\ &= 0. \end{aligned}$$

This completes the proof. □

We end up this section with several remarks on Theorem 2.1.

Remark 2.1. (i) The representation (2.7) obviously fulfills the symmetry $p^s(x, z) = p^s(z, x)$ for all $z, x \in \mathbb{R}^3 \setminus Y$.

- (ii) Theorem 2.1 is equivalent to the formula derived from the Foldy-Lax method [15]. In fact, in the Foldy model the scattered field takes the form (see e.g., [8, 9] or [10, Section 2.1])

$$p^s(x, z) = \sum_{m,j=1}^N a_j [\tilde{\Theta}^{-1}]_{m,j} \Phi_k(x, y_m) \Phi_k(y_j, z), \quad x, z \in \mathbb{R}^3 \setminus Y, \quad x \neq z, \quad (2.13)$$

where the entries of the matrix $\tilde{\Theta}$ are given by

$$\tilde{\Theta}_{m,j} = \begin{cases} -a_j \Phi_k(y_m, y_j), & m \neq j, \\ 1, & m = j. \end{cases} \quad (2.14)$$

Comparing (2.14), (2.13) with (2.6), (2.7) we may find the following relation between α_j and the scattering coefficient a_j involved in the Foldy model:

$$a_j = -\frac{1}{ik/(4\pi) - \alpha_j}, \quad j = 1, 2, \dots, N.$$

- (iii) It is emphasized that the multiple scattering between the point-like scatterers has been taken into account in (2.7). In the Born approximation case, i.e., $\min_{1 \leq i, j \leq N} |y_i - y_j| \gg \lambda := \omega/(2\pi)$, the scattered field can be approximated by

$$p^s(x, z) = -\sum_{j=1}^N \frac{1}{ik/(4\pi) - \alpha_j} \Phi_k(y_j, z) \Phi_k(x, y_j), \quad x, z \in \mathbb{R}^3 \setminus Y.$$

In the special case of a single scatterer, i.e., $Y = \{y_1\}$, we have

$$p(x, z) = \Phi_k(x, z) - \frac{1}{ik/(4\pi) - \alpha_1} \Phi_k(y_1, z) \Phi_k(x, y_1), \quad x \in \mathbb{R}^3, \quad x \neq y, \quad x \neq z.$$

2.2 Inverse scattering with near-field data measured on spheres

Assume there is *a priori* information that all point scatterers are contained in B_R for some $R > 0$. In this section we consider the inverse problem of locating the positions y_j from the near-field data $\cup_{j=1}^M \{p^s(x, z_j) : x \in \Gamma_R\}$ generated by M incident point sources $z_j \in \Gamma_R$.

In contrast to the far-field response matrix corresponding to incident plane waves (see [8, 9, 27]), the near-field response matrix $\tilde{\mathbf{N}} \in \mathbb{C}^{M \times M}$, with the entries defined by

$$\tilde{\mathbf{N}}_{m,j} = p^s(x_m, z_j), \quad m, j = 1, 2, \dots, M,$$

cannot be decomposed into the form $\tilde{\mathbf{N}} = \mathbf{H}^* \Theta^{-1} \mathbf{H}$ in a straightforward way. Here $(\cdot)^*$ denotes the adjoint of an operator or the transpose conjugate of a matrix. In fact, it holds that $\tilde{\mathbf{N}} = \mathbf{H} \Theta^{-1} \mathbf{H}$ with the matrix \mathbf{H} defined later in (2.18). This leads to difficulties in applying the MUSIC algorithm to the near-field case. Motivated by the ideas of [21], we

apply the so-called outgoing-to-incoming (OtI) operator T to both sides of (2.7), in order to get an "indirect" factorization of the form $T\tilde{\mathbf{N}} = \mathbf{H}^* \Theta^{-1} \mathbf{H}$. Below we state the definition of the OtI mapping. Recall that $h_n^{(1)}$ are the spherical Bessel functions of the first kind of order n , and Y_n^m are the spherical harmonics of order n .

Definition 2.1. Let $f = p^s|_{\Gamma_R}$, where p^s is an outgoing radiation solution with the expansion

$$p^s(x) = \sum_{n=0}^{\infty} \sum_{m=-n}^n p_{n,m} h_n^{(1)}(k|x|) Y_n^m(\hat{x}), \quad p_{n,m} \in \mathbb{C}, \quad \text{in } |x| \geq R.$$

Then the outgoing-to-incoming mapping is defined as $Tf = \tilde{p}^s|_{\Gamma_R}$, with

$$\tilde{p}^s(x) = - \sum_{n=0}^{\infty} \sum_{m=-n}^n p_{n,m} \overline{h_n^{(1)}(k|x|) Y_n^m(\hat{x})}, \quad |x| \geq R. \tag{2.15}$$

In this paper we shall use the following properties of T (see [21]).

Lemma 2.1. (i) $T(\Phi_k(\cdot, y)|_{\Gamma_R}) = \overline{\Phi_k(\cdot, y)}|_{\Gamma_R}$ for $|y| < R$.

(ii) T can be extended to a bounded, linear and one-to-one mapping $T : L^2(\Gamma_R) \rightarrow L^2(\Gamma_R)$ with a dense range.

(iii) An explicit representation of T is given by

$$(Tg)(x) = \int_{\Gamma_R} K(x, y) g(y) ds(y) \quad \text{for } g \in L^2(\Gamma_R) \tag{2.16}$$

with the kernel

$$K(x, y) := - \frac{1}{4\pi R^2} \sum_{n=0}^{\infty} \left(\frac{\overline{h_n^{(1)}(kR)}}{h_n^{(1)}(kR)} \right) (2n+1) P_n(\cos\theta). \tag{2.17}$$

In (2.17), P_n are the Legendre polynomials and θ denotes the angle between $x, y \in \Gamma_R$.

Following the way processed in [29, Chapter 4.1], we propose a modified MUSIC algorithm to characterize the point-like scatterers Y from the near-field measurement $p^s(x, z_j)|_{\Gamma_R}$, $j = 1, 2, \dots, M$. We assume $M > N$, i.e., the number of incident point sources is larger than the number of point scatterers. Then by Lemma 2.1 (i) and the definition of T ,

$$(Tp^s)(x, z_j) = - \sum_{m,j=1}^N \left[\Theta^{-1}(k, \alpha) \right]_{m,j} \Phi_k(y_l, z_j) \overline{\Phi_k(x, y_m)} \quad \text{for } 1 \leq j \leq M.$$

We emphasize that, for fixed z_j , the data $p^s(x, z_j)$ for all $x \in \Gamma_R$ are needed in order to calculate $(Tp^s)(x, z_j)$ through (2.16). Then we define the modified near-field response matrix $\mathbf{N} \in \mathbb{C}^{M \times M}$ by

$$\mathbf{N}_{ij} = (Tp^s)(z_i, z_j) \quad \text{for } z_i, z_j \in \Gamma_R, \quad i, j = 1, \dots, M.$$

and define the matrix $\mathbf{H} \in \mathbb{C}^{N \times M}$ as

$$\mathbf{H}_{mi} = \Phi_k(y_m, z_i), \quad m = 1, 2, \dots, N, \quad i = 1, 2, \dots, M. \tag{2.18}$$

Thus \mathbf{N} can be decomposed into the form

$$\mathbf{N} = -\mathbf{H}^* \Theta^{-1} \mathbf{H},$$

with the adjoint $\mathbf{H}^* \in \mathbb{C}^{M \times N}$. Since $M > N$, the locations y_m are such that \mathbf{H} has maximal rank N . Then by a standard argument from linear algebra, the ranges $\mathcal{R}(\mathbf{H}^*)$ and $\mathcal{R}(\mathbf{N})$ coincide. For any point $z \in \mathbb{R}^3$ we define the vector $\phi_z \in \mathbb{C}^M$ by

$$\phi_z = \left(\overline{\Phi_k(z_1, z)}, \overline{\Phi_k(z_2, z)}, \dots, \overline{\Phi_k(z_M, z)} \right)^T.$$

The main result of this section is stated as following.

Theorem 2.2. *Let $\{z_n, n \in \mathbb{N}\} \subset \Gamma_R$ be a countable set of points such that any analytic function on Γ_R that vanishes on z_n for all $n \in \mathbb{N}$ vanishes identically. Let K_Y be a compact subset of \mathbb{R}^3 containing all y_m . Then there exists $M_0 \in \mathbb{N}$ such that for any $M \geq M_0$ the following characterization holds for every $z \in K_Y$:*

$$z \in Y \iff \phi_z \in \mathcal{R}(\mathbf{N}) \iff \mathbf{P}\phi_z = 0,$$

where $\mathbf{P}: \mathbb{C}^M \rightarrow \mathcal{R}(\mathbf{N})^\perp = \text{Ker}(\mathbf{N}^*)$ is the orthogonal projection onto the null space $\text{Ker}(\mathbf{N}^*)$ of \mathbf{N}^* .

Proof. We modify the idea in the proof of [29, Theorem 4.1] to be applicable to the near-field case. First we note that if $z \in Y$, then $\phi_z \in \mathcal{R}(\mathbf{H}^*)$ because $\phi_{y_m}, m = 1, \dots, N$ are the columns of the matrix $\mathbf{H}^* \in \mathbb{C}^{M \times N}$.

We show now that there exists $M_0 \in \mathbb{N}$ such that the vectors $(\phi_{y_1}, \phi_{y_2}, \dots, \phi_{y_N}, \phi_z)$ are linearly independent for all $M \geq M_0$ and all points $z \in K_Y \setminus Y$. In particular, this would imply that \mathbf{H}^* has maximal rank N and that $\phi_z \notin \mathcal{R}(\mathbf{H}^*)$ for all $z \in K_Y \setminus Y$. Assume on the contrary that this is not the case. Then there exist sequences $M_l \rightarrow \infty$ and $\{z^{(l)}\} \subset K_Y \setminus Y$ and $\{\lambda^{(l)}\} \subset \mathbb{C}^N$ and $\{\mu^{(l)}\} \subset \mathbb{C}$ such that

$$|\mu^{(l)}| + \sum_{n=1}^N |\lambda_n^{(l)}| = 1,$$

and

$$\mu^{(l)} \overline{\Phi_k(z_j, z^{(l)})} + \sum_{n=1}^N \lambda_n^{(l)} \overline{\Phi_k(z_j, y_n)} = 0 \quad \text{for } j=1, 2, \dots, M_l,$$

or equivalently,

$$\overline{\mu^{(l)}} \Phi_k(z_j, z^{(l)}) + \sum_{n=1}^N \overline{\lambda_n^{(l)}} \Phi_k(z_j, y_n) = 0 \quad \text{for } j=1, 2, \dots, M_l. \tag{2.19}$$

Since all the sequences are bounded, there exist converging subsequences $z^{(l)} \rightarrow z \in K_Y$ and $\overline{\lambda_n^{(l)}} \rightarrow \lambda_n^0 \in \mathbb{C}^N$ and $\overline{\mu^{(l)}} \rightarrow \mu^0 \in \mathbb{C}$ as $l \rightarrow \infty$. We fix $j \in \mathbb{N}$ and let l tend to infinity. Then

$$|\mu^0| + \sum_{n=1}^N |\lambda_n^0| = 1 \quad \text{and} \quad \mu^0 \Phi_k(z_j, z) + \sum_{n=1}^N \lambda_n^0 \Phi_k(z_j, y_n) = 0 \quad \text{for all } j \in \mathbb{N}. \tag{2.20}$$

We conclude from the assumption on the "richness" of the set $\{z_n : n \in \mathbb{N}\} \subset \Gamma_R$ that

$$\mu^0 \Phi_k(x, z) + \sum_{n=1}^N \lambda_n^0 \Phi_k(x, y_n) = 0 \quad \text{for all } x \in \Gamma_R.$$

Therefore, by Rellich's Lemma and unique continuation,

$$\mu^0 \Phi_k(x, z) + \sum_{n=1}^N \lambda_n^0 \Phi_k(x, y_n) = 0 \quad \text{for all } x \notin \{z, y_1, y_2, \dots, y_N\}.$$

Now, we distinguish between two cases:

Case (a): Let $z \notin \{y_1, y_2, \dots, y_N\}$. By letting x tend to z and to $y_n, n = 1, 2, \dots, N$ we conclude that all coefficients μ^0 and $\lambda_n^0, n = 1, 2, \dots, N$ have to vanish. This contradicts the first equation of (2.20).

Case (b): Let $z \in \{y_1, y_2, \dots, y_N\}$. Without loss of generality we assume that $z = y_1$. By the same arguments as in case (a) we conclude that

$$\mu^0 + \lambda_1^0 = 0 \quad \text{and} \quad \lambda_n^0 = 0 \quad \text{for } n = 2, \dots, N. \tag{2.21}$$

Now we write (2.19) in the form, for $j = 1, 2, \dots, M_l$,

$$\left[\overline{\mu^{(l)}} + \overline{\lambda_1^{(l)}} \right] \Phi_k(z_j, y_1) + \overline{\mu^{(l)}} \left[\Phi_k(z_j, z^{(l)}) - \Phi_k(z_j, y_1) \right] + \sum_{n=2}^N \overline{\lambda_n^{(l)}} \Phi_k(z_j, y_n) = 0. \tag{2.22}$$

Note that

$$\rho_l = \left| \overline{\mu^{(l)}} + \overline{\lambda_1^{(l)}} \right| + \sum_{n=2}^N \left| \overline{\lambda_n^{(l)}} \right| + |z^{(l)} - y_1| \rightarrow 0 \quad \text{as } l \rightarrow \infty.$$

By Taylor’s formula we have that

$$\Phi_k(z_j, z^{(l)}) - \Phi_k(z_j, y_1) = (z^{(l)} - y_1) \cdot (y_1 - z_j) \frac{ik|z_j - y_1| - 1}{|z_j - y_1|^2} \Phi_k(z_j, y_1) + \mathcal{O}(|z^{(l)} - y_1|^2),$$

as l tends to ∞ . Division of (2.22) by ρ_l yields

$$\left[\tilde{\lambda}_1^{(l)} - a^{(l)} \cdot (z_j - y_1) \frac{\overline{\mu^{(l)}}(ik|z_j - y_1| - 1)}{|z_j - y_1|^2} \right] \Phi_k(z_j, y_1) + \sum_{n=2}^N \tilde{\lambda}_n^{(l)} \Phi_k(z_j, y_n) = \mathcal{O}(|z^{(l)} - y_1|),$$

for all $j = 1, 2, \dots, M_l$ where

$$\tilde{\lambda}_1^{(l)} = \frac{\overline{\mu^{(l)}} + \overline{\lambda_1^{(l)}}}{\rho_l}, \quad \tilde{\lambda}_n^{(l)} = \frac{\overline{\lambda_n^{(l)}}}{\rho_l}, \quad n = 2, \dots, N, \quad a^{(l)} = \frac{z^{(l)} - y_1}{\rho_l}.$$

These sequences are all bounded as well, i.e., we can extract further subsequences $\tilde{\lambda}_n^{(l)} \rightarrow \tilde{\lambda}_n^0$ for $n = 1, 2, \dots, N$ and $a^{(l)} \rightarrow a \in \mathbb{R}^3$ as $l \rightarrow \infty$. We have that

$$\sum_{n=1}^N |\tilde{\lambda}_n^0| + |a| = 1, \tag{2.23}$$

and

$$\left[\tilde{\lambda}_1^0 - a \cdot (z_j - y_1) \frac{\mu^0(ik|z_j - y_1| - 1)}{|z_j - y_1|^2} \right] \Phi_k(z_j, y_1) + \sum_{n=2}^N \tilde{\lambda}_n^0 \Phi_k(z_j, y_n) = 0,$$

for all $j \in \mathbb{N}$. Again, by the assumption on the set $\{z_n, n \in \mathbb{N}\} \subset \Gamma_R$ we conclude that this equation holds for all $x \in \Gamma_R$, i.e.,

$$\tilde{\lambda}_1^0 \Phi_k(x, y_1) + \mu^0 a \cdot \nabla \Phi_k(x, y_1) + \sum_{n=2}^N \tilde{\lambda}_n^0 \Phi_k(x, y_n) = 0 \quad \text{for all } x \in \Gamma_R.$$

Then by Rellich’s Lemma and unique continuation again,

$$\tilde{\lambda}_1^0 \Phi_k(x, y_1) + \mu^0 a \cdot \nabla \Phi_k(x, y_1) + \sum_{n=2}^N \tilde{\lambda}_n^0 \Phi_k(x, y_n) = 0 \quad \text{for all } x \notin Y.$$

Then letting x tend to $y_n, n = 1, 2, \dots, N$ we conclude that $\mu^0 a = 0, \tilde{\lambda}_n^0 = 0, n = 1, 2, \dots, N$. We recall from (2.20) and (2.21) that $|\mu^0| = 1/2$ and thus $a = 0$. This, finally, contradicts (2.23). \square

Now we choose M incident point sources z_j to be uniformly distributed on Γ_R . It is easy to see that the assumption on z_j in Theorem 2.2 is satisfied as M tends to infinity.

Denote by $\{\psi_j\}_{j=1}^M$ the orthonormal basis of the matrix $\mathbf{N} \in \mathbb{C}^{M \times M}$. By Theorem 2.2 we have

$$z \in Y \iff W(z) := \frac{1}{|\mathbf{P}\phi_z|} > 0, \quad \mathbf{P}\phi_z = \phi_z - \sum_{j=1}^M (\phi_z \cdot \bar{\psi}_j) \psi_j.$$

Hence the values of $W(y_j)$, $j = 1, 2, \dots, M$, should be considerably larger than those of $W(z)$, $z \in \mathbb{R}^3 \setminus Y$. In the following we apply the MUSIC to recover N point-like scatterers by sending M incident point source waves. We take $k = 5$, which implies the wavelength $\lambda = 2\pi/k \approx 1.256$. The reconstruction results are all from perturbation data of the near field measurements by the multiplication of $(1 + \delta\zeta)$ at the noise level $\delta = 10\%$. Here ζ is a Gaussian random number between 1 and -1 . In our numerical experiments, we will locate the following points

$$Y = \begin{cases} \{(0, -1), (0, 0.5), (1, 1)\}, & \text{if } N = 3, \\ \{(0, -1), (0, 0.5), (1, 1), (-1, 1), (-1, 1), (1, -1)\}, & \text{if } N = 6. \end{cases}$$

It is assumed that the point sources and receivers are located at Γ_R with $R = 5$, and that 128 near-field data are observed on Γ_R . In Fig. 1, the scattering coefficients are set uniformly as $\alpha_j = 1$ and the scatterers are located by sending 10 incident point sources (i.e. $M = 10$) from the polluted near-field data. In Fig. 2, we test the sensitivity of the resolution with respect to the number of incident point sources, and find that the inverse solution can be improved by increasing the number of incident point source wave. In Fig. 3 (a) and (b), 128 receivers and 16 incident point sources are located on an ellipse with the semi-major axis $a = 4$ and semi-minor axis $b = 3$. We used the scheme proposed in [37] to compute the Otl mapping defined on a non-spherical measurement surface. In Fig. 3 (c) and (d), the scatterers are illuminated by 16 point sources located only at the upper-half part of the ellipse. That is why the inverse solutions have been distorted. The unpolluted near-field data taken on the ellipse corresponding to 10 point source waves are sufficient to precisely locate these scatterers.

3 Inverse scattering by extended solid and point scatterers immersed in a fluid

The aim of this section is to investigate the multi-scale inverse scattering problem of finding the shape of an unknown extended elastic body and the location of several point scatterers immersed in a fluid. Due to the existence of the extended scatterer, we shall use the near-field data incited by infinitely many point source waves.

3.1 Mathematical formulations

The forward scattering problem can be formulated as an interaction problem between acoustic and elastic waves on the interface of the extended elastic body together with a

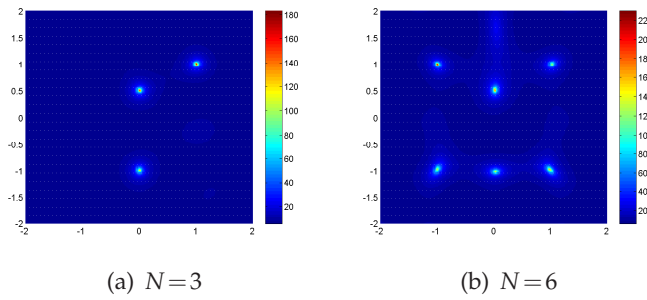


Figure 1: Reconstruction of N point-like scatterers using MUSIC algorithm with $\alpha_j=1$ and $M=10$.

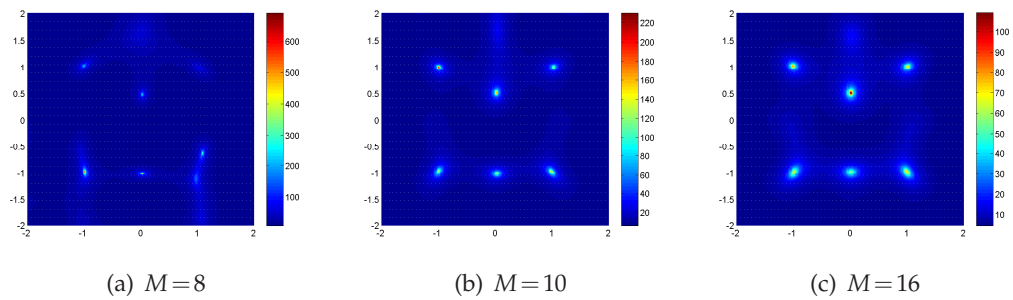


Figure 2: Reconstruction of 6 point-like scatterers with different number (M) of incident point sources. $\alpha_j=1, j=1, 2, \dots, 6$.

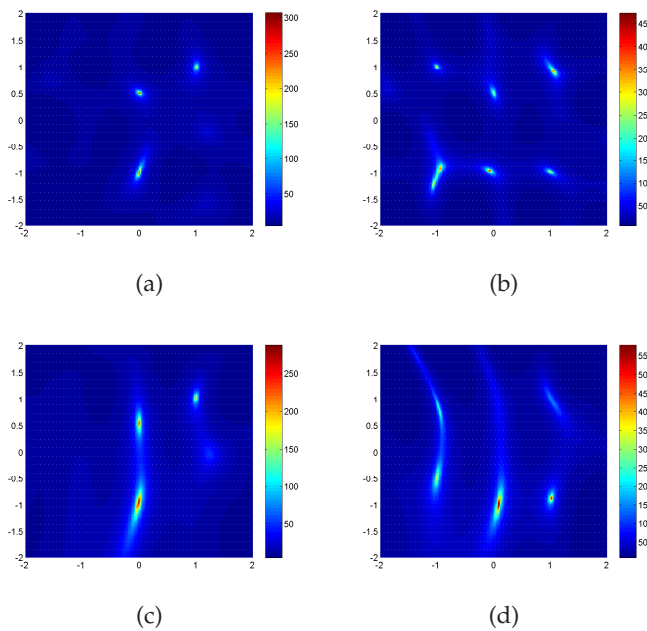


Figure 3: Incident point sources are emitted from a closed ellipse in (a) and (b), and from only the upper-half part of the ellipse in (c) and (d).

multi-scattering problem between the extended and point-like scatterers. Let $\Omega \subset \mathbb{R}^3$ be a bounded domain with the C^2 -smooth boundary Γ and denote by ν the unite normal vector to Γ directed into the exterior of Ω . We assume that Ω is occupied by an isotropic linearly elastic solid characterized by the real-valued constant mass density $\rho > 0$ and the Lamé constants $\lambda, \mu \in \mathbb{R}$ satisfying $\mu > 0, 3\lambda + 2\mu > 0$. The exterior $\Omega^c := \mathbb{R}^3 \setminus \overline{\Omega}$ is assumed to be connected. Again denote by $Y = \{y_1, \dots, y_N\}$, $y_j \in \Omega^c := \mathbb{R}^3 \setminus \overline{\Omega}$, $j = 1, 2, \dots, N$, the set of the positions of point scatterers. It is supposed that the elastic body Ω together with the point scatterers are immersed in a homogeneous compressible inviscid fluid with the constant mass density $\rho_f > 0$.

In the following we rigorously formulate the forward scattering of time-harmonic point source waves by the scatterer $\Omega \cup Y$. Let $k = \omega/c > 0$ be the wave number of the fluid, where $\omega > 0$ denotes the frequency of the time harmonic incoming wave and $c > 0$ the sound speed. Following the notation in Section 2, let $p^i = p^i(\cdot, z)$ be an incident point source located at $z \in \mathbb{R}^3 \setminus \{\Omega \cup Y\}$. Under the hypothesis of small amplitude oscillations both in the solid and the fluid, the direct or forward scattering problem can be formulated as the following boundary value problem (see e.g., [18, 33]): determine the displacement $u(\cdot, z) \in H^1(\Omega)^3$ and the total field $p(\cdot, z) = p^i(\cdot, z) + p^s(\cdot, z) \in H^1_{loc}(\mathbb{R}^3 \setminus \{\Omega \cup Y \cup \{z\}\})$ such that

$$\Delta^* u + \rho\omega^2 u = 0 \quad \text{in } \Omega, \quad \Delta^* := \mu\Delta + (\lambda + \mu)\nabla\nabla\cdot, \tag{3.1}$$

$$\Delta p + k^2 p = 0 \quad \text{in } \mathbb{R}^3 \setminus \{\overline{\Omega} \cup Y \cup \{z\}\}, \tag{3.2}$$

$$\eta u \cdot \nu = \partial_\nu p \quad \text{on } \Gamma, \quad \eta = \rho_f \omega^2 > 0, \tag{3.3}$$

$$\mathbf{T}u = -\nu p \quad \text{on } \Gamma, \tag{3.4}$$

and that the following boundary conditions across y_j hold

$$(\Gamma_2 p)_j = \alpha_j (\Gamma_1 p)_j, \quad \alpha_j \in \mathbb{C}, \quad j = 1, 2, \dots, N. \tag{3.5}$$

Here, $\partial_\nu p = \nu \cdot \nabla p$ denotes the normal derivative of p on Γ , the operators Γ_j ($j = 1, 2$) are defined as in (2.5), \mathbf{T} stands for the standard stress operator defined by

$$\mathbf{T}u = 2\mu\partial_\nu u + \lambda\nu(\nabla \cdot u) + \mu\nu \times (\nabla \times u) \quad \text{on } \Gamma. \tag{3.6}$$

Furthermore, the scattered field p^s is required to fulfill the Sommerfeld radiation condition (2.2).

It is well known [26, 36] that, for certain geometries and some frequencies, the problem (3.1)-(3.4) (i.e., $Y = \emptyset$) is not always uniquely solvable due to the occurrence of so-called traction free oscillations. We call $\omega \in \mathbb{R}$ a Jones frequency if the system

$$\Delta^* u_0 + \rho\omega^2 u_0 = 0 \quad \text{in } \Omega, \quad \mathbf{T}u_0 = 0, \quad u_0 \cdot \nu = 0 \quad \text{on } \Gamma,$$

admits a nontrivial solution. Throughout this section we suppose that ω is not a Jones

frequency. Hence the transmission problem

$$\Delta^* u_0 + \rho\omega^2 u_0 = 0 \quad \text{in } \Omega, \tag{3.7}$$

$$\Delta p_0^s + k^2 p_0^s = 0 \quad \text{in } \Omega^c, \tag{3.8}$$

$$\eta u_0 \cdot \nu - \partial_\nu p_0^s = f \quad \text{on } \Gamma, \tag{3.9}$$

$$\mathbf{T}u_0 + \nu p_0^s = h \quad \text{on } \Gamma, \tag{3.10}$$

with p_0^s satisfying the Sommerfeld radiation condition, has a unique solution $(p_0^s, u_0) \in H^1_{loc}(\Omega^c) \times H^1(\Omega)^3$ for all $f \in H^{-1/2}(\Gamma)$, $h \in H^{-1/2}(\Gamma)^3$; see [34, Theorem 3.3]. Given an incident point source $p^i(x, z)$, we denote by $p_0(x, z) = p^i(x, z) + p_0^s(x, z)$ and $u_0(x, z)$ the unique solution corresponding to (3.1)-(3.4) in the absence of the point scatterers. Then $p_0^s(x, z)$ and $u_0(x, z)$ solve the problem (3.7)-(3.10) with $f = \partial_\nu p^i(\cdot, z)|_\Gamma$, $h = -\nu p^i(\cdot, z)|_\Gamma$.

To state the well-posedness of our multiscale scattering problem, we introduce the matrix $\mathcal{M} = \mathcal{M}(\omega, \alpha) \in \mathbb{C}^{N \times N}$ with the entries defined by

$$[\mathcal{M}(\omega, \alpha)]_{n,j} = \begin{cases} p_0^s(y_n, y_j) + \Phi_k(y_n, y_j), & n \neq j, \\ p_0^s(y_j, y_j) + \frac{ik}{4\pi} - \alpha_j, & n = j, \end{cases} \quad n, j = 1, 2, \dots, N, \tag{3.11}$$

and let

$$S'_\alpha = \{\omega > 0 : \det(\mathcal{M}(\omega, \alpha)) = 0\}.$$

Analogously to Theorem 2.1, we have

Theorem 3.1. *There exists at most one solution $(u, p^s) \in H^1(\Omega)^3 \times H^1_{loc}(\Omega^c \setminus \{Y \cup \{z\}\})$ to the problem (3.1)-(3.5), provided that ω is not a Jones frequency and $\text{Im} \alpha_j \leq 0$ for all $j = 1, 2, \dots, N$. Moreover, if $\omega \notin S'_\alpha$, this unique solution is of the form*

$$p^s(x, z) = p_0^s(x, z) - \sum_{m,j=1}^N [\mathcal{M}^{-1}(\omega, \alpha)]_{m,j} p_0(y_j, z) p_0(x, y_m), \tag{3.12}$$

$$u(x, z) = u_0(x, z) - \sum_{m,j=1}^N [\mathcal{M}^{-1}(\omega, \alpha)]_{m,j} p_0(y_j, z) u_0(x, y_m). \tag{3.13}$$

Proof. The uniqueness follows from the fact that ω is not a Jones frequency and the same argument as in the proof of Theorem 2.1. It remains to check that the solution $(p^s(x, z), u(x, z))$ given by (3.12) and (3.13) satisfies the problem (3.1)-(3.5) if $\omega \notin S'_\alpha$. Clearly, u and p^s are solutions to the Navier equation in Ω and the Helmholtz equation in $\Omega^c \setminus Y$, respectively. The transmission conditions (3.3)-(3.4) can be verified directly from (3.9)-(3.10) with $f = \partial_\nu p^i(\cdot, z)|_\Gamma$, $h = -\nu p^i(\cdot, z)|_\Gamma$. Furthermore, the impedance-type conditions (3.5) across y_j follow from (2.12) and the definition of $\mathcal{M}(\omega, \alpha)$; see Lemma 3.1 below for a proof in the general case. □

Remark 3.1. (i) If the extended scatterer is absent, i.e., $\Omega = \emptyset$, we have $p_0^s \equiv 0, u_0 \equiv 0$ and thus $p_0 = p^i = \Phi_k(\cdot, z)$. The expression (3.12) then reduces to (2.7) for the point interaction model. If $Y = \emptyset$, it is obvious that $p^s = p_0^s, u = u_0$.

(ii) Both p^s and u consist of two parts. The first part, p_0^s resp. u_0 , is due to the scattering from the extended scatterer. The second part is a linear combination of interactions between the point-like scatterers and the interaction between the point-like obstacle with the extended one.

Now we turn to studying the inverse problem of detecting $\Omega \cup Y$ from the near-field data $\{p^s(x, z) : x, z \in \Gamma_R\}$ corresponding to infinitely many point sources at a fixed frequency. Here, we choose $R > 0$ sufficiently large such that the $\Omega \cup Y \subset B_R$. Our goal is to verify the factorization scheme with near-field data generated by point source waves for the two-scale model (3.1)-(3.5). In particular, we unify the MUSIC algorithm for the point-interaction model in Section 2 and the factorization method with far-field patterns corresponding to a single extended elastic body (see [30]). The essence of this approach is to properly factorize the near-field operator $\mathcal{N} : L^2(\Gamma_R) \rightarrow L^2(\Gamma_R)$, defined by

$$(\mathcal{N}\varphi)(x) = \int_{\Gamma_R} p^s(x, z) \varphi(z) ds(z) \quad \text{for } x \in \Gamma_R. \quad (3.14)$$

A "direct" factorization of the near-field operator yields to the relation $\mathcal{N} = GJ'G'$ where the adjoint G' of G would be defined via a bilinear form other than sesquilinear form (see [29, Chapter 1.7] for the discussions in acoustic scattering). This is similar to the factorization $\tilde{\mathbf{N}} = \mathbf{H}\Theta^{-1}\mathbf{H}$ of the near-field response matrix for the point-interaction model (cf. Section 2.2), and thus leads to essential difficulties in the characterization of the scatterer $\Omega \cup Y$ through the eigensystem of \mathcal{N} . As seen in Section 2.2, it is necessary to apply the outgoing-to-incoming operator T to (3.14), in order to get an "indirect" factorization form $T\mathcal{N} = (TG)J^*(TG)^*$ with the adjoint G^* of G defined via the sesquilinear form. Here J and G are referred to as the middle operator and solution operator to be defined later.

3.2 Auxiliary boundary value problems

We first introduce several auxiliary boundary value problems. For $h \in H^{1/2}(\Gamma)$, consider the boundary value problem of finding a solution $w \in H^1(\Omega)$ such that

$$\Delta w + k^2 w = 0 \quad \text{in } \Omega, \quad w = h \quad \text{on } \Gamma. \quad (3.15)$$

The above problem is uniquely solvable if k^2 is not a Dirichlet eigenvalue of $-\Delta$ in Ω . The normal derivative of w on Γ defines the interior Dirichlet-Neumann map $\Lambda : H^{1/2}(\Gamma) \rightarrow H^{-1/2}(\Gamma)$ by $h \mapsto \partial_\nu w|_\Gamma$ where w is the unique solution to problem (3.15). With the definition of Λ , we introduce the second auxiliary boundary value problem as follows: given

$f \in H^{1/2}(\Gamma)$ and $\mathbf{c} = (c_1, c_2, \dots, c_N) \in \mathbf{C}^N$, find $u \in H^1(\Omega)^3$ and $p^s \in H^1_{loc}(\Omega^c \setminus Y)$ such that

$$\Delta^* u + \rho \omega^2 u = 0 \quad \text{in } \Omega, \tag{3.16}$$

$$\Delta p^s + k^2 p^s = 0 \quad \text{in } \Omega^c \setminus Y, \tag{3.17}$$

$$\eta u \cdot \nu - \partial_\nu p^s = \Lambda f \quad \text{on } \Gamma, \tag{3.18}$$

$$\mathbf{T}u + \nu p^s = -\nu f \quad \text{on } \Gamma, \tag{3.19}$$

$$(\Gamma_2 p^s)_j - \alpha_j (\Gamma_1 p^s)_j = c_j \quad j = 1, 2, \dots, N, \tag{3.20}$$

and that p^s satisfies the Sommerfeld radiation condition. We state the well-posedness of solutions to the previous boundary value problem in Lemma 3.1.

Lemma 3.1. *Suppose that $\omega \notin S'_\alpha$, $\text{Im} \alpha_j \leq 0$ and that ω is not a Jones frequency. Then the unique solution of (3.16)-(3.20) takes the form*

$$p^s(x) = p^s_f(x) - \sum_{m,j=1}^N [\mathcal{M}^{-1}]_{m,j} \left((p^s_f(y_j) - c_j) p_0(x, y_m) \right), \quad x \in \Omega^c \setminus Y, \tag{3.21}$$

$$u(x) = u_f(x) - \sum_{m,j=1}^N [\mathcal{M}^{-1}]_{m,j} \left((p^s_f(y_j) - c_j) u_0(x, y_m) \right), \quad x \in \Omega. \tag{3.22}$$

Here, $(p^s_f, u_f) \in H^1_{loc}(\Omega^c) \times H^1(\Omega)^3$ is the unique solution of (3.16)-(3.19) without fulfilling the boundary condition (3.20) (i.e., $Y = \emptyset$), and analogously, $(p_0(x, z), u_0(x, z)) \in H^1_{loc}(\Omega^c \setminus \{z\}) \times H^1(\Omega)^3$ is the unique solution of (3.1)-(3.4) when $Y = \emptyset$.

Proof. Observe that $(p_0(x, z), u_0(x, z))$ satisfies the homogeneous coupling conditions

$$\eta u_0 \cdot \nu - \partial_\nu p_0 = 0 \quad \mathbf{T}u_0 + \nu p_0 = 0 \quad \text{on } \Gamma.$$

By Theorem 3.1, we only need to check the conditions in (3.20). For simplicity we write $L_j[f] = (\Gamma_2 f)_j - \alpha_j (\Gamma_1 f)_j$. Since $p^s_f(x)$ is analytic at y_m and $p_0(x, y_m) = p^s_0(x, y_m) + \Phi_k(x, y_m)$, straightforward calculations show that

$$L_l[p^s_f] = p^s_f(y_l), \quad L_l[p_0(\cdot, y_m)] = [\mathcal{M}]_{m,l}, \quad l, m = 1, 2, \dots, N.$$

Hence by (3.21),

$$\begin{aligned} L_l[p^s(x)] &= L_l[p^s_f(x)] - \sum_{m,j=1}^N [\mathcal{M}^{-1}]_{m,j} \left((p^s_f(y_j) - c_j) L_l[p_0(x, y_m)] \right) \\ &= p^s_f(y_l) - \sum_{m,j=1}^N \left((p^s_f(y_j) - c_j) [\mathcal{M}^{-1}]_{m,j} [\mathcal{M}]_{l,j} \right) \\ &= c_l. \end{aligned}$$

This completes the proof. □

Remark 3.2. Our two-scale scattering problem can be equivalently formulated as the boundary value problem (3.16)-(3.20), if we take

$$f := \Phi_k(\cdot, z)|_\Gamma, \quad c_j := -[(\Gamma_2 \Phi_k(\cdot, z))_j - \alpha_j (\Gamma_1 \Phi_k(\cdot, z))_j] = -\Phi_k(y_j, z) \tag{3.23}$$

for some $z \in \Omega^c \setminus \mathcal{Y}$. With the boundary data (3.23), we have $p_f^s = p_0^s(\cdot, z)$, $u_f = u_0(\cdot, z)$ and $p_f^s(y_j) - c_j = p_0(y_j, z)$. Hence the expressions in Lemma 3.1 are identical with those in Theorem 3.1.

To justify the factorization method, we still need to consider the interior transmission problem of finding $u \in H^1(\Omega)^3$ and $w \in H^1(\Omega)$ such that

$$\Delta^* u + \rho \omega^2 u = 0 \quad \text{in } \Omega, \tag{3.24}$$

$$\Delta w + k^2 w = 0 \quad \text{in } \Omega, \tag{3.25}$$

$$\eta u \cdot \nu - \partial_\nu w = h \quad \text{on } \Gamma, \tag{3.26}$$

$$\mathbf{T}u + \nu w = g \quad \text{on } \Gamma, \tag{3.27}$$

with $h \in H^{-1/2}(\Gamma)$, $g \in H^{-1/2}(\Gamma)^3$. We call ω an interior transmission eigenvalue if there exists a non-trivial pair $(w, u) \in H^1(\Omega) \times H^1(\Omega)^3$ satisfying the system (3.24)-(3.27) with $h = g = 0$. We refer to [30] for a discussion of the discreteness of the interior transmission eigenvalues. In the present study we assume that ω is not an interior transmission eigenvalue, so that the problem (3.16)-(3.19) admits a unique solution (see [34]).

3.3 Factorization of near-field operator

The radiation solution p^s to the problem (3.16)-(3.20) defines the solution operator

$$G(f, \mathbf{c}) = p^s|_{\Gamma_R}, \quad H^{1/2}(\Gamma) \times \mathbb{C}^N \rightarrow L^2(\Gamma_R). \tag{3.28}$$

Introduce the incidence function as

$$(Hg)(x) = \int_{\Gamma_R} \Phi_k(x, y) g(y) ds(y), \quad x \in \mathbb{R}^3, \quad g \in L^2(\Gamma_R).$$

The incidence operator $\mathcal{H}: L^2(\Gamma_R) \rightarrow H^{1/2}(\Gamma) \times \mathbb{C}^N$ is defined by

$$\mathcal{H}g := (Hg|_\Gamma, \mathbf{c}), \quad \mathbf{c} = (c_1, \dots, c_N), \quad L^2(\Gamma_R) \rightarrow H^{1/2}(\Gamma) \times \mathbb{C}^N, \tag{3.29}$$

where

$$c_j = -[(\Gamma_2 Hg)_j - \alpha_j (\Gamma_1 Hg)_j] = -(Hg)(y_j).$$

It easily follows that $\mathcal{N} = G\mathcal{H}$ since $\Lambda(Hg|_\Gamma) = \partial_\nu(Hg)|_\Gamma$. We now recall the single layer potential operator S and its discrete analogue K by

$$(S\varphi)(x) = \int_\Gamma \Phi_k(x, y) \varphi(y) ds(y), \quad x \in \mathbb{R}^3 \setminus \Gamma, \quad \varphi \in H^{-1/2}(\Gamma),$$

$$(K(\mathbf{b}))(x) = \sum_{j=1}^N b_j \Phi_k(x, y_j), \quad x \neq y_j, \quad \mathbf{b} = (b_1, b_2, \dots, b_N) \in \mathbb{C}^N,$$

and define $\mathcal{S}(\varphi, \mathbf{b}) := S(\varphi) - K(\mathbf{b})$ which is a radiation solution to the Helmholtz equation in $\Omega^c \setminus Y$. Denote by (u, v) is the unique solution of (3.24)-(3.27) with $h = \partial_\nu(\mathcal{S}(\varphi, \mathbf{b}))^+|_\Gamma$ and $g = -\nu(\mathcal{S}(\varphi, \mathbf{b}))^+|_\Gamma$, where the superscripts $(\cdot)^\pm$ stand for the limits taking from outside and inside, respectively. Introduce the operator $\mathcal{J}: H^{-1/2}(\Gamma) \times \mathbb{C}^N \rightarrow H^{1/2}(\Gamma) \times \mathbb{C}^N$ as following:

$$\mathcal{J}(\varphi, \mathbf{b}) = (v|_\Gamma, \mathbf{a}), \quad a_j = (\Gamma_2 \mathcal{S}(\varphi, \mathbf{b}))_j - \alpha_j (\Gamma_1 \mathcal{S}(\varphi, \mathbf{b}))_j.$$

Setting $\tilde{p}^s = \mathcal{S}(\varphi, \mathbf{b})|_{\Omega^c \setminus Y}$, it follows that

$$\Delta^* u + \rho \omega^2 u = 0 \quad \text{in } \Omega, \tag{3.30}$$

$$\Delta \tilde{p}^s + k^2 \tilde{p}^s = 0 \quad \text{in } \Omega^c \setminus Y, \tag{3.31}$$

$$\eta u \cdot \nu - \partial_\nu \tilde{p}^s = \Lambda(v|_\Gamma) \quad \text{on } \Gamma, \tag{3.32}$$

$$\mathbf{T}u + \nu \tilde{p}^s = -\nu v \quad \text{on } \Gamma, \tag{3.33}$$

$$(\Gamma_2 \tilde{p}^s)_j - \alpha_j (\Gamma_1 \tilde{p}^s)_j = a_j \quad j = 1, 2, \dots, N. \tag{3.34}$$

Hence, from the definition of \mathcal{J} we see

$$\begin{aligned} G\mathcal{J}(\varphi, \mathbf{b}) &= G(v|_\Gamma, \mathbf{a}) = [S(\varphi) - K(\mathbf{b})](x) \\ &= \int_\Gamma \Phi_k(x, y) \varphi(y) ds(y) - \sum_{j=1}^N b_j \Phi_k(x, y_j), \quad x \in \Gamma_R. \end{aligned}$$

On the other hand, the adjoint operator $\mathcal{H}^*: H^{-1/2}(\Gamma) \times \mathbb{C}^N \rightarrow L^2(\Gamma_R)$ is given by

$$(\mathcal{H}^*(\varphi, \mathbf{b}))(x) = \int_\Gamma \overline{\Phi_k(x, y)} \varphi(y) ds(y) - \sum_{j=1}^N b_j \overline{\Phi_k(x, y_j)}, \quad x \in \Gamma_R.$$

Comparing the previous two identities and applying the OtI mapping T (see Definition 2.1 or Lemma 2.1 (i)) yield $\mathcal{H}^* = TG\mathcal{J}$. Therefore, we obtain $\mathcal{H} = \mathcal{J}^*(TG)^*$ and the factorization

$$T\mathcal{N} = TG\mathcal{H} = G\mathcal{J}^*G^* \quad \text{with } G := TG. \tag{3.35}$$

3.4 Inversion algorithm and numerical examples

We collect properties of the solution operator G and the middle operator \mathcal{J} in the following two lemmas.

Lemma 3.2. (i) *The adjoint $G^*: L^2(\Gamma_R) \rightarrow H^{-1/2}(\Gamma) \times \mathbb{C}^N$ is injective, taking the form*

$$G^* = (G_0^* - B^*P, P).$$

Here, $G_0: H^{1/2}(\Gamma) \rightarrow L^2(\Gamma_R)$ is the solution operator in the absence of the point scatterers (i.e., $Y = \emptyset$) and the mapping $P: H^{-1/2}(\Gamma) \rightarrow \mathbb{C}^N$ is defined by

$$Pg = \left\{ \sum_{m=1}^N [\mathcal{M}^{-1}]_{j,m} \int_{\Gamma_R} \overline{p_0(x, y_m)} g(x) ds(x) : j=1, 2, \dots, N \right\}.$$

The operator $B: H^{1/2}(\Gamma) \rightarrow \mathbb{C}^N$ maps the boundary data f to the restriction of p_f^s to Y , i.e.,

$$Bf = \{p_f^s(y_1), p_f^s(y_2), \dots, p_f^s(y_N)\} \in \mathbb{C}^N.$$

(ii) The operators G and \mathbb{G} are both compact with dense ranges in $L^2(\Gamma_R)$.

(iii) For $z \in B_R$, the function $\phi_z(\cdot) = \overline{\Phi_k(\cdot, z)}|_{\Gamma_R}$ belongs to the range of \mathbb{G} if and only if $z \in \Omega \cup Y$.

Proof. (i) By the definition of G , G_0 and B , we have for $(f, \mathbf{c}) \in H^{-1/2}(\Gamma) \times \mathbb{C}^N$ that

$$G(f, \mathbf{c}) = G_0 f - \sum_{m,j=1}^N [\mathcal{M}^{-1}]_{m,j} [(Bf)_j - c_j] p_0(x, y_m), \quad x \in \Gamma_R.$$

Here $(Bf)_j$ denotes the j -th element of $Bf \in \mathbb{C}^N$. Given $g \in L^2(\Gamma_R)$, it follows using the symmetry of \mathcal{M} and the definition of P that

$$\begin{aligned} \langle G(f, \mathbf{c}), g \rangle_{L^2(\Gamma_R)} &= \langle G_0 f, g \rangle_{L^2(\Gamma_R)} + \langle \mathbf{c}, Pg \rangle_{\mathbb{C}^N} - \langle Bf, Pg \rangle_{\mathbb{C}^N} \\ &= \langle f, (G_0^* - B^* P)g \rangle_{L^2(\Gamma_R)} + \langle \mathbf{c}, Pg \rangle_{\mathbb{C}^N}. \end{aligned}$$

This proves the expression of G^* . If $G^*g = 0$, then $Pg = 0$ and thus $G_0^*g = 0$. It is known that G_0^* is injective (see [37]), hence G^* is also injective.

(ii) The compactness of G follows from the boundedness of $G: H^{1/2}(\Gamma) \times \mathbb{C}^N \rightarrow H^{1/2}(\Gamma_R)$ and the compact imbedding of $H^{1/2}(\Gamma_R)$ into $L^2(\Gamma_R)$. The denseness of G and \mathbb{G} follows from the assertion (i) and the unitarity of T .

(iii) The third one can be treated analogously to [10, Lemma 4.5]. Assume first $z \in \Omega \cup Y$. Let (u, w) be the solution of (3.24)-(3.27) with

$$f = \partial_\nu \Phi_k(\cdot, z)|_\Gamma \in H^{-1/2}(\Gamma), \quad g = -\nu \Phi_k(\cdot, z) \in H^{-1/2}(\Gamma)^3.$$

It follows that $\Lambda(w|_\Gamma) = \partial_\nu w|_\Gamma$ by the definition Λ . Hence the solution $(u, \Phi_k(\cdot, z))$ solves problem (3.16)-(3.20) with $f = w|_\Gamma$ and

$$c_j = (\Gamma_2 \Phi_k(x, z))_j - \alpha_j (\Gamma_1 \Phi_k(x, z))_j, \quad j = 1, 2, \dots, N.$$

Together with the definition of G , this gives the relation

$$\mathbb{G}(f, \mathbf{c}) = T(\Phi_k(\cdot, z)|_{\Gamma_R}) = \overline{\Phi_k(\cdot, z)}|_{\Gamma_R} = \phi_z,$$

implying that $\phi_z \in \text{Range}(\mathbb{G})$.

On the other hand, let $z \in B_R$ and assume that there exists $f \in H^{1/2}(\Gamma)$ and $\mathbf{c} \in \mathbb{C}^N$ such that $\mathbb{G}(f, \mathbf{c}) = \phi_z$. Then, $G(f, \mathbf{c}) = \Phi_k(\cdot, z)|_{\Gamma_R}$. Let (u, p^s) be the unique solution to (3.16)-(3.20) with the same f and \mathbf{c} . It holds that $p^s = \Phi_k(\cdot, z)$ in $\Omega^c \setminus Y$ due to Rellich's identity and the unique continuation of solutions to the Helmholtz equation. If $z \in \Omega^c \setminus Y$, the boundedness of $\lim_{x \rightarrow z} p^s(x)$ contradicts the singularity of $\Phi_k(x, z)$ at $x = z$. If $z \in \Gamma$, the relation $p^s \in H^{1/2}(\Gamma)$ contradicts to the fact that $\Phi_k(\cdot, z) \notin H^{1/2}(\Gamma)$. Hence, $z \in \Omega \cup Y$. \square

The properties of the middle operator \mathcal{J} are summarized as following.

Lemma 3.3. *Assume that k^2 is not a Dirichlet eigenvalue of $-\Delta$ in Ω , ω is neither a Jones frequency nor an interior transmission eigenvalue, and that the matrixes Θ and \mathcal{M} are both invertible and $\text{Im} \alpha_j \leq 0$ for all $j = 1, 2, \dots, N$. Then*

- (i) *The operator $\mathcal{J} : H^{-1/2}(\Gamma) \times \mathbb{C}^N \rightarrow H^{1/2}(\Gamma) \times \mathbb{C}^N$ is injective.*
- (ii) *There exists a self-adjoint and coercive operator $\mathcal{J}_0 : H^{-1/2}(\Gamma) \times \mathbb{C}^N \rightarrow H^{1/2}(\Gamma) \times \mathbb{C}^N$ such that $\mathcal{J} - \mathcal{J}_0 : H^{-1/2}(\Gamma) \times \mathbb{C}^N \rightarrow H^{1/2}(\Gamma) \times \mathbb{C}^N$ is compact.*
- (iii) *$\text{Im} \langle (\varphi, \mathbf{b}), \mathcal{J}(\varphi, \mathbf{b}) \rangle > 0$ for all $(\varphi, \mathbf{b}) \in H^{-1/2}(\Gamma) \times \mathbb{C}^N$ with $\varphi \neq 0$ and $b_j \neq 0$.*

To prove Lemma 3.3, one needs to combine the argument in the proof of [22, Lemma 4.8] for a two-scale acoustic scattering problem and that of [37, Lemma 3.10] where the fluid-solid interaction problem with a single extended solid was treated. For brevity we omit the proof here. The properties of G and \mathcal{J} allow us to apply the range identity of [21, Theorem 2.15] to the factorization form established in (3.35). Consequently, the ranges of \mathbb{G} and $(T\mathcal{N})_{\sharp} := |\text{Re}(T\mathcal{N})| + |\text{Im}(T\mathcal{N})|$ coincide. In view of Lemma 3.2, the range of $T\mathcal{N}$ can be used to characterize the scatterer $\Omega \cup Y$. As a consequence of Picard's range criterion, we obtain the following sufficient and necessary computational criterion for precisely characterizing $\Omega \cup Y$ through the eigensystem of $T\mathcal{N}$.

Theorem 3.2. *Let $\phi_z(\cdot) = \overline{\Phi_k(\cdot, z)}|_{\Gamma_R}$ for $z \in B_R$. Denote by $\lambda_j \in \mathbb{C}$ the eigenvalues of the operator $(T\mathcal{N})_{\sharp}$ with the corresponding normalized eigenfunctions $\varphi_j \in L^2(\Gamma_R)$. Then*

$$z \in \Omega \cup Y \iff \phi_z \in (T\mathcal{N})_{\sharp}^{1/2} \iff W(z) := \left[\sum_j \frac{|(\phi_z, \varphi_j)_{L^2(\Gamma_R)}|^2}{\lambda_j} \right]^{-1} > 0.$$

Theorem 3.2 was justified in [37] when $Y = \emptyset$. It provides a new computational criterion for characterizing the positions of point scatterers if $\Omega = \emptyset$. If the extended obstacle is absent, we consider the problem

$$\Delta p^s + k^2 p^s = 0 \quad \text{in } \Omega^c \setminus Y, \quad (\Gamma_2 p^s)_j - \alpha_j (\Gamma_1 p^s)_j = c_j, \quad \alpha_j \in \mathbb{C}, j = 1, 2, \dots, N, \quad (3.36)$$

where p^s satisfies the Sommerfeld radiation condition. The corresponding solution operator $\tilde{G} : \mathbb{C}^N \rightarrow L^2(\Gamma_R)$, defined by $\tilde{G}\mathbf{c} = p^s|_{\Gamma_R}$, can be factorized as $T\tilde{G} = -\mathbf{H}\Theta^{-1}\mathbf{H}^*$, where T is

the OtI mapping and both \mathbf{H} and Θ^{-1} are finite dimensional matrices. If $\text{Im}\alpha_j \leq 0$ and Θ is invertible, Theorems 3.2 and 3.3 both apply to the matrices \mathbf{H} and Θ^{-1} in the finite space \mathbb{C}^N . What differs from the MUSIC algorithm is that, the eigensystem of the near response matrix rather than its orthonormal basis is involved in Theorem 3.2. Hence, the MUSIC algorithm for point scatterers and the factorization method for extended obstacles have been unified in Theorem 3.2 for the two-scale scattering problem.

In the following numerical experiments, we want to determine a kite-shaped solid surrounded by N point-like obstacles. The boundary of the extended scatterer is parameterized by (see Fig. 4)

$$x(t) = (\cos t + 0.65 \sin(2t) - 0.65, 1.5 \sin t), \quad t \in [0, 2\pi).$$

We set $k=5$, $\omega=3$, $\mu=2$, $\lambda=1$, $\rho_f=1$ and $\rho=2$. We use 64 incident point sources and 64 observations points uniformly distributed at Γ_R with $R=5$. In Fig. 5, the point-like scatterers are chosen to equivalently lie on the line segment $\{(x_1, x_2) \in \mathbb{R}^2: x_1 = -4, x_2 \in [-3, 3]\}$. The "impedance coefficients" are uniformly taken as $\alpha_j = 1$, $j = 1, 2, \dots, N$. The number of the point scatterers is set as $N=5$ in Fig. 5 (a) and (d), $N=7$ in Fig. 5 (b) and (e), and $N=13$ in Fig. 5 (c) and (f), respectively. The inverse solution reconstructed from perturbed data at the noise level 2% are presented in Fig. 5 (g)-(i). The indicator functions are visualized from the direction $(0,0,1)$ in Fig. 5 (a)-(c), where the configuration of the extended scatterer can be seen clearly. However, the point-like obstacles can be visualized only from the XY-plane shown in Fig. 5 (d)-(f), because we have used unpolluted synthetic near-field data generated by (3.12) and (3.13). In the noisy case, the image of the extended scatterer is distorted and unreliable, while the point-like obstacles cannot be distinguished if they are getting too closed (see Fig. 5 (i)). The validity of our inversion algorithm is confirmed again in Fig. 6, where the extended scatterer together with N point scatterers equivalently lying on a circle are reconstructed. Finally we test the sensitivity of the factorization method to the values of the "impedance" coefficients α_j .

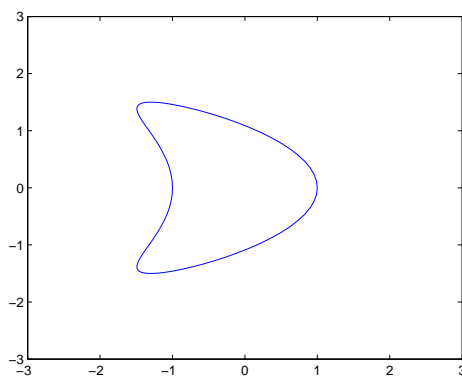


Figure 4: The Kite-shaped extended obstacle.

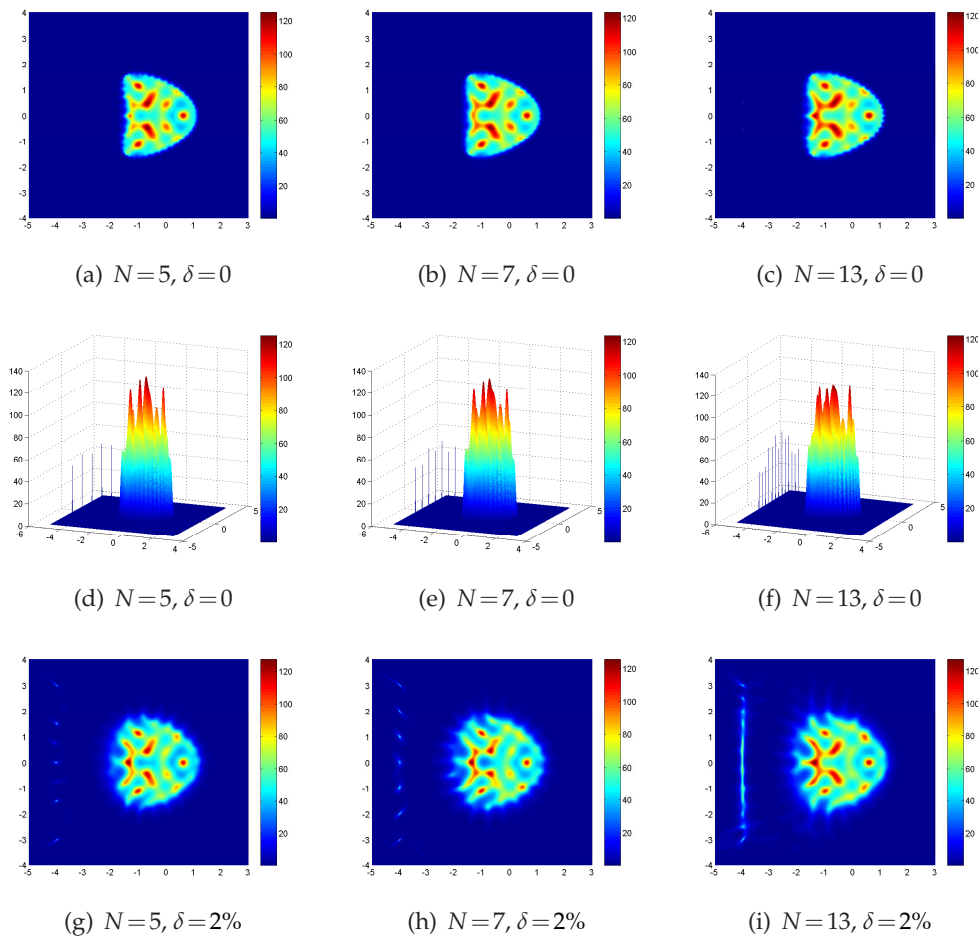


Figure 5: Reconstruction of kite-shaped extended obstacle and N point-like scatterers lying on the line segment $\{(x_1, x_2) \in \mathbb{R}^2 : x_1 = -4, x_2 \in [-3, 3]\}$ with $\alpha_j = 1$.

We fix one point-like obstacle at $(2.5, 2.5)$, and set $\alpha_1 = 10$ in Fig. 7 (a) and (d), $\alpha_1 = 1$ in Fig. 7 (b) and (e), $\alpha_1 = 0.05$ in Fig. 7 (c) and (f). It can be observed that the values of the indicator function around the point-like obstacle grow as the value of α_j decreases. In other words, the point-like obstacle is more visible for small α_1 . This is due to the fact that the diagonal terms of the middle matrices \mathcal{M}^{-1} and Θ^{-1} are inversely proportional to α_j .

Acknowledgments

The work of T. Yin is partially supported by Chongqing University Postgraduates' Science and Innovation Fund (CDJXS12101108), the China Scholarship Council and the

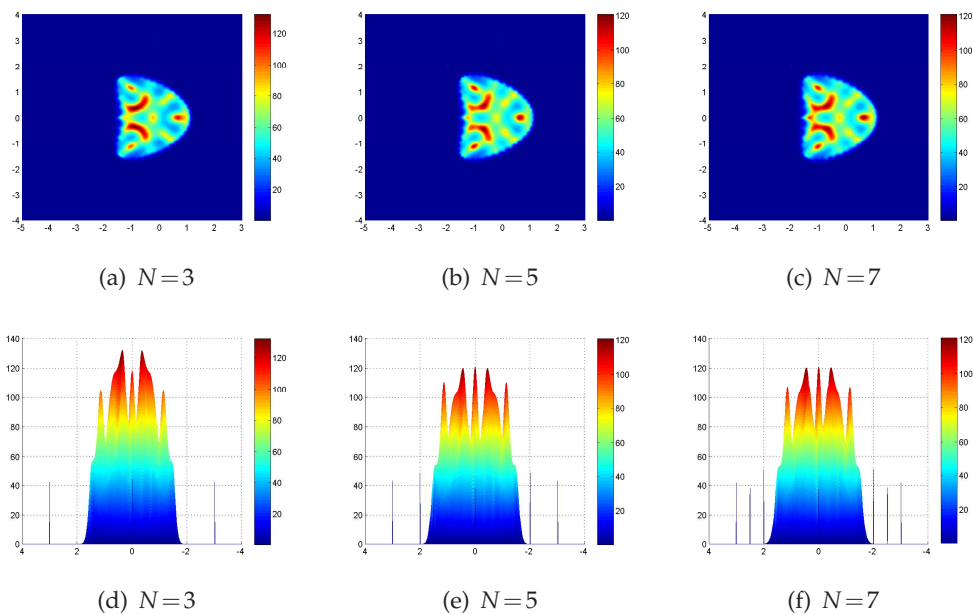


Figure 6: Reconstruction of kite-shaped extended obstacle and N point-like scatterers lying around with $\alpha_j=1$.

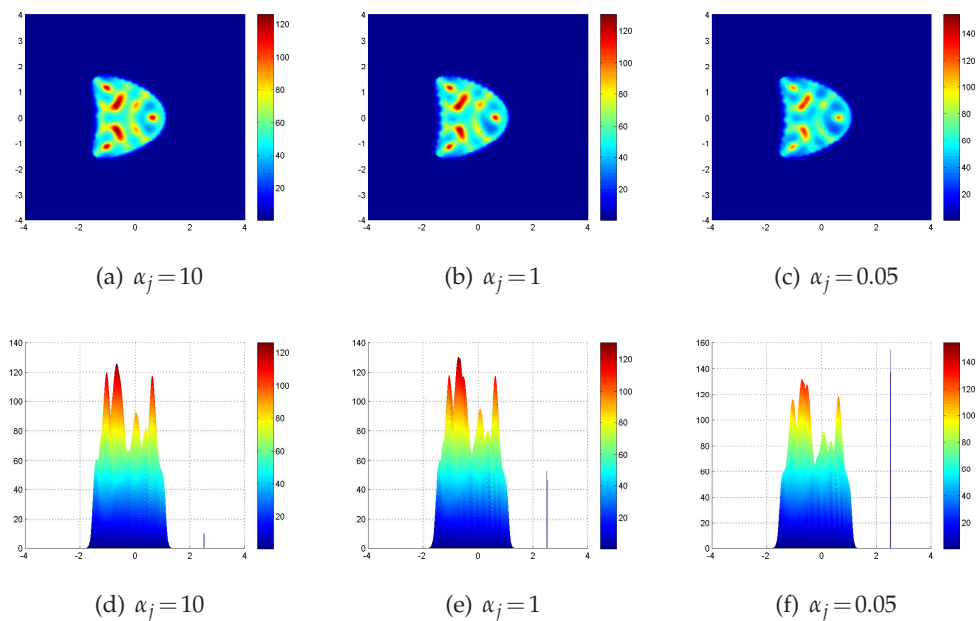


Figure 7: Reconstruction of the kite-shaped extended obstacle and one point-like scatterer with different scattering coefficients.

NSFC Grant (11371385). The work of L. Xu is partially supported by the NSFC Grant (11371385), the Start-up fund of Youth 1000 plan of China and that of Youth 100 plan of Chongqing University.

References

- [1] S. Albeverio and P. Kurasov, Singular Perturbations of Differential Operators, in Solvable Schrödinger Type Operators, London Math. Soc. Lecture Note Ser. 271, Cambridge University Press, Cambridge, UK, 2000.
- [2] S. Albeverio and K. Pankrashkin, A remark on Krein's resolvent formula and boundary conditions *J. Phys. A*, 38 (2005), 4859–4864.
- [3] H. Ammari and H. Kang, Boundary layer techniques for solving the Helmholtz equation in the presence of small inhomogeneities, *J. Math. Anal. Appl.*, 296 (2004), 190–208.
- [4] H. Ammari and H. Kang, Reconstruction of Small Inhomogeneities from Boundary Measurements, Lecture Notes in Mathematics 1846, Springer-Verlag, Berlin, 2004.
- [5] G. Bao, K. Huang, P. Li and H. Zhao, A direct imaging method for inverse scattering using the Generalized Foldy-Lax formulation, *Contemp. Math.*, 615 (2014), 49–70.
- [6] G. Bao and P. Li, Numerical solution of inverse scattering for near-field optics, *Optics Letters*, 32 (2007), 1465–1467.
- [7] M. Cheney, The linear sampling method and the music algorithm, *Inverse Problems*, 17 (2001), 591–596.
- [8] D. P. Challa and M. Sini, Inverse scattering by point-like scatterers in the Foldy regime, *Inverse Problems*, 28 (2012), 125006.
- [9] D. P. Challa and M. Sini, On the justification of the Foldy-Lax approximation for the acoustic scattering by small rigid bodies of arbitrary shapes, *Multiscale Model. Simul.*, 12 (2014), 55–108.
- [10] D. P. Challa, G. Hu and M. Sini, Multiple scattering of electromagnetic waves by a finite number of point-like obstacles, *Mathematical Models and Methods in Applied Sciences*, 24 (2014), 863–899.
- [11] D. Colton, and R. Kress, *Inverse Acoustic and Electromagnetic Scattering Theory*, Berlin, Springer, 1998.
- [12] A.J. Devaney, Super-resolution processing of multi-static data using time reversal and MUSIC, available at www.ece.neu.edu/faculty/devaney (2000).
- [13] J. Elschner, G. C. Hsiao and A. Rathsfeld, An inverse problem for fluid-solid interaction, *Inverse Problems and Imaging*, 2 (2008), 83–120.
- [14] J. Elschner, G. C. Hsiao and A. Rathsfeld, An optimization method in inverse acoustic scattering by an elastic obstacle, *SIAM J. Appl. Math.*, 70 (2009), 168–187.
- [15] L. L. Foldy, The multiple scattering of waves. I., General theory of isotropic scattering by randomly distributed scatterers, *Phys. Rev.*, 2 (1945), 107–119.
- [16] F. K. Gruber, E. A. Marengo and A. J. Devaney, Time-reversal imaging with multiple signal classification considering multiple scattering between the targets, *J. Acoust. Soc. Am.*, 115 (2004), 3042-3047.
- [17] S. Hou, K. Solna and H. Zhao, A direct imaging algorithm for extended targets, *Inverse Problems*, 22 (2006), 1151–1178.
- [18] G. C. Hsiao, R. E. Kleinman and G. F. Roach, Weak solution of fluid-solid interaction problem, *Math. Nachr.*, 218 (2000), 139–163.

- [19] G. Hu, J. Li, H. Liu and H. Sun, Inverse elastic scattering for multiscale rigid bodies with a single far-field measurement, *SIAM Journal on Imaging Sciences*, 6 (2014), 2285–2309.
- [20] G. Hu, J. Li and H. Liu, Recovering complex elastic scatterers by a single far-field pattern, *Journal of Differential Equation*, 257 (2014), 469–489.
- [21] G. Hu, J. Yang, B. Zhang and H. Zhang, Near-field imaging of scattering obstacles via the factorization method, *Inverse Problems*, 30, 095005.
- [22] G. Hu, A. Mantile and M. Sini, Direct and inverse acoustic scattering by a collection of extended and point-like scatterers, *Multiscale Modeling and Simulation*, 12 (2014), 996–1027.
- [23] K. Huang and P. Li, A two-scale multiple scattering problem, *Multiscale Model. Simul.*, 8 (2010), 1511–1534.
- [24] K. Huang, P. Li and H. Zhao, An efficient algorithm for the generalized Foldy- Lax formulation, *J. Comput. Phys.*, 234 (2013), 376–398.
- [25] K. Ito, B. Jin and J. Zou, A direct sampling method to an inverse medium scattering problem, *Inverse Problems*, 28 (2012), 025003.
- [26] D. S. Jones, Low-frequency scattering by a body in lubricated contact, *Quart. J. Mech. Appl. Math.*, 36 (1983), 111–137.
- [27] A. Kirsch, The music algorithm and the factorization method in inverse scattering theory for inhomogeneous media, *Inverse Problems*, 18 (2002), 1025–1040.
- [28] A. Kirsch, Characterization of the shape of a scattering obstacle using the spectral data of the far field operator, *Inverse Problems*, 14 (1998), 1489–1512.
- [29] A. Kirsch and N. Grinberg, *The Factorization Method for Inverse Problems*, New York, Oxford Univ. Press, 2008.
- [30] A. Kirsch and A. Ruiz, The factorization method for an inverse fluid-solid interaction scattering problem, *Inverse Problems and Imaging*, 6 (2012), 681–695.
- [31] P. Kurasov and A. Posilicano, Finite speed of propagation and local boundary conditions for wave equations with point interactions, *Proc. Amer. Math. Soc.*, 133 (2005), 3071–3078.
- [32] J. Li, H. Liu and Q. Wang, Locating multiple multi-scale electromagnetic scatterers by a single far-field measurement, *SIAM J. Imaging Sci.*, 6 (2013), 2285–2309.
- [33] C. J. Luke and P. A. Martin, Fluid-solid interaction: Acoustic scattering by a smooth elastic obstacle, *SIAM Appl. Math.*, 55 (1995), 904–922.
- [34] P. Monk and V. Selgas, An inverse fluid-solid interaction problem, *Inverse Probl. Imaging*, 3 (2009), 173–198.
- [35] P. Monk and V. Selgas, Near field sampling type methods for the inverse fluid-solid interaction problem, *Inverse Problems and Imaging*, 5 (2011), 465–483.
- [36] D. Natroshvili, G. Sadunishvili, I. Sigua, Some remarks concerning Jones eigenfrequencies and Jones modes, *Georgian Mathematical Journal*, 12 (2005), 337–348.
- [37] T. Yin, G. Hu, L. Xu and B. Zhang, Near-field imaging of scattering obstacles with the factorization method II: Fluid-solid interaction, submitted. Available at: <http://www.wias-berlin.de/people/hu/home.html>
- [38] H. Zhao, Analysis of the response matrix for an extended target, *SIAM Appl. Math.*, 64 (2004), 725–745.